nature biotechnology

A calcium- and light-gated switch to induce gene expression in activated neurons

Dongmin Lee[1–3,5], Jung Ho Hyun[1,5], Kanghoon Jung[1], Patrick Hannan[1] & Hyung-Bae Kwon[1,4]

Despite recent advances in optogenetics, it remains challenging to manipulate gene expression in specific populations of neurons. We present a dual-protein switch system, Cal-Light, that translates neuronal-activity-mediated calcium signaling into gene expression in a light-dependent manner. In cultured neurons and brain slices, we show that Cal-Light drives expression of the reporter EGFP with high spatiotemporal resolution only in the presence of both blue light and calcium. Delivery of the Cal-Light components to the motor cortex of mice by viral vectors labels a subset of excitatory and inhibitory neurons related to learned lever-pressing behavior. By using Cal-Light to drive expression of the inhibitory receptor halorhodopsin (eNpHR), which responds to yellow light, we temporarily inhibit the lever-pressing behavior, confirming that the labeled neurons mediate the behavior. Thus, Cal-Light enables dissection of neural circuits underlying complex mammalian behaviors with high spatiotemporal precision.

Identifying a specific neuronal ensemble underlying an animal behavior is crucial for understanding normal brain function. However, selective labeling of circuits is difficult because action potential pulses are too transient to be monitored over a long period of time and brain activity is quite noisy. Recent development of genetically encoded calcium indicators (GECIs) allow monitoring of changes in neuronal activity in real-time with cellular resolution, but the brain regions that can be monitored are limited (for example, one focal plane of superficial layer of cortex). Furthermore, activation of GECIs is not linked with gene expression.

Immediate early genes (IEGs), such as *c-Fos* (also known as *Fos*) and *Arc*, and its derivatives (ESARE, RAM) have been widely used to label and manipulate active neuronal ensembles[1–10]. However, IEG expression is derived from a variety of signaling pathways originating from a rise in Ca^{2+} and the second-messenger cyclic AMP[11]. As a result, gene expression is not tightly associated with neuronal firing and temporal resolution is poor[12].

The calcium integrator named CaMPARI (calcium-modulated photoactivatable ratiometric integrator)[13] uses irreversible photoconversion of EOS fluorescent protein upon elevated Ca^{2+} and violet light, such that a group of active neurons can be visualized at a specific time point with high temporal resolution. However, CaMPARI only allows visualization of an activity snapshot, but because it does not link neuronal activity with gene expression, the approach enables investigation of correlations and not causal relationships between neuronal function and behavior. These limitations have hampered the application of these methodologies to label and control the neural circuits responsible for complex behaviors.

We sought to develop an optogenetic system to label an active population of neurons with high temporal precision. In an initial pilot screen, we tested over 300 constructs that differed in their light-sensitive proteins and calcium sensors, linker type and size, and the order of individual protein domains. In brief, we tested various light-inducible gene expression systems such as cryptochrome 2 (CRY2)–CRY-interacting basic-helix-loop-helix 1 (CRY2-CIBN) linked to split Cre recombinase[14] and the LOV domain–helix-turn-helix (LOV-HTH) system[15] (**Supplementary Figs. 1** and **2**). All of the systems we tested showed weak Ca^{2+} or light dependency or displayed partial responsiveness to light. The most probable reason for these drawbacks is a spatial mismatch between the signal cue and the reporter (i.e., the activity-driven Ca^{2+} rise occurs in the cytosol despite gene transcription happening in the nucleus). To solve this problem, we designed a special protein encoder to efficiently translate cytosolic Ca^{2+} events into gene expression in the nucleus. We tethered tetracycline-controlled transcriptional activator (tTA) to the outer cellular membrane, limiting spontaneous gene expression. Then, we fused tTA to tobacco etch virus protease (TEVp) cleavage sequence (TEVseq), and made TEVseq cleavage dependent on blue light. To achieve this, we engineered a Jα-helix of *Avena sativa* phototropin 1 light-oxygen-voltage 2 domains (AsLOV2)[16] to be released upon blue light exposure. We hid TEVseq within the C terminus of Jα-helix so TEVseq would be recognized by TEV protease only in the presence of blue light (**Fig. 1a**). To make the system Ca^{2+}-dependent, we split TEVp into N- and C-terminal fragments (TEV-N and TEV-C) that could regain protease activity upon binding of calcium sensors (calmodulin (CaM) and M13) following a Ca^{2+} rise in the cytosol (**Fig. 1a**).

In short, Cal-Light consists of two synthetic proteins (**Fig. 1a**). The first protein is made of five different protein domains as follows: a transmembrane (TM) domain, CaM, TEV- N, TEVseq inserted into a truncated form of AsLOV2, and tTA. The second protein is a fusion between M13 and TEV-C. In this configuration, neuronal activity increases cytosolic Ca^{2+} levels causing M13 to bind to CaM. The M13–CaM interaction brings TEV-C closer to TEV-N, permitting

[1]Max Planck Florida Institute for Neuroscience, Jupiter, Florida, USA. [2]Department of Anatomy, College of Medicine, Korea University, Seoul, Republic of Korea. [3]Department of Biomedical Science, Brain Korea 21 PLUS, College of Medicine, Korea University, Seoul, Republic of Korea. [4]Max Planck Institute of Neurobiology, Martinsried, Germany. [5]These authors contributed equally to this work. Correspondence should be addressed to H.-B.K. (hyungbae.kwon@mpfi.org).

Received 28 November 2016; accepted 17 May 2017; published online 26 June 2017; doi:10.1038/nbt.3902

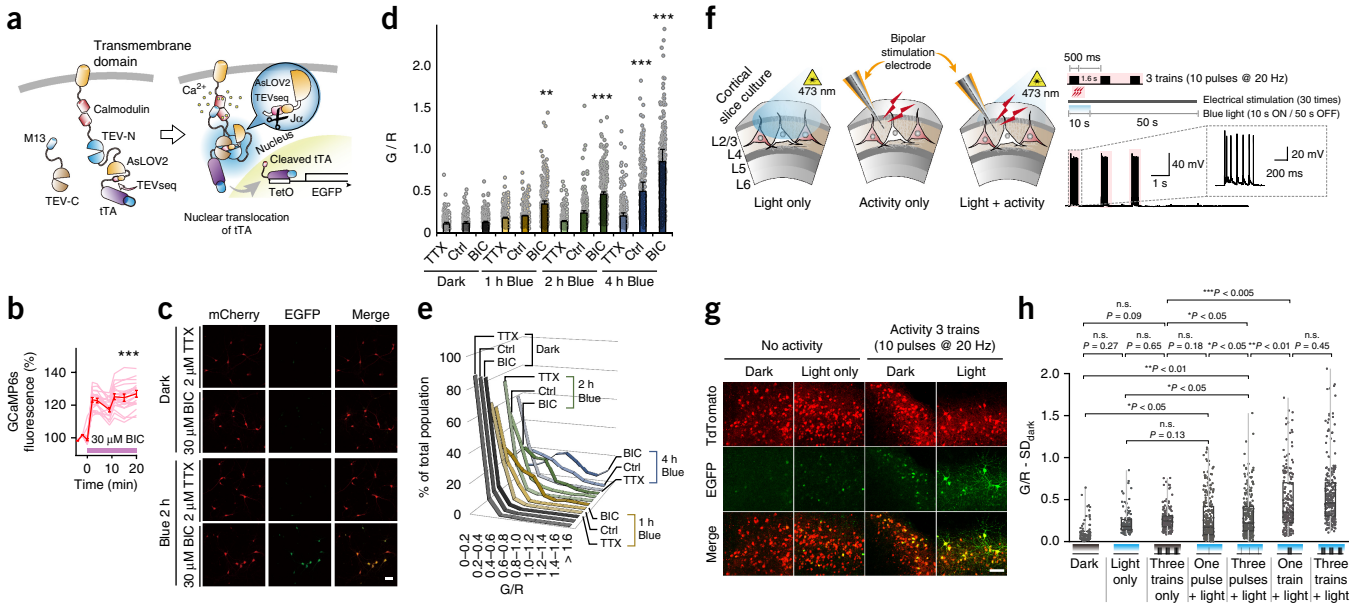

Figure 1 Development and verification of Cal-Light. (**a**) Schematic drawing of Cal- Light. M13 and CaM proteins are fused to C terminus and N terminus of TEV protease (TEV-C and TEV-N), respectively. When Ca^{2+} arises in the cytosol, M13 and CaM bind to each other and subsequently TEV-C and TEV-N regain proteolytic functions. However, TEV protease cannot recognize TEVseq easily in a dark condition, because TEVseq is inserted at the C terminus of AsLOV2 Jα-helix. Blue light causes a conformational change in the Jα- helix, making TEVseq unmasked. Cleaved tTA translocates to the nucleus and initiates gene expression. (**b**) GCaMP6s responses before and after 30 μM bicuculline in hippocampal culture neurons. (**c**) Cal-Light constructs were transfected to hippocampal culture neurons, and EGFP reporter gene expression was monitored in light and dark conditions and in the presence or absence of bicuculline. Note that EGFP expression occurred only when both blue light was illuminated and activity was increased. Scale bar, 100 μm. TTX, tetrodotoxin; BIC, bicuculline. (**d**) Summary graph of light- and activity-dependent gene expression. Intermittent flash of blue light (1 s ON/9 s OFF) for 1, 2, and 4 h. G/R ratio was calculated from individual cells. Dark TTX: 0.112 ± 0.019, n = 190 neurons; Dark Ctrl: 0.117 ± 0.019, n = 169 neurons; Dark BIC: 0.129 ± 0.015, n = 185 neurons; 1 h Blue TTX: 0.180 ± 0.011, n = 193 neurons; 1 h Blue Ctrl: 0.208 ± 0.007, n = 160 neurons; 1 h Blue BIC: 0.350 ± 0.036, n = 211 neurons; 2 h Blue TTX: 0.141 ± 0.011, n = 187 neurons; 2 h Blue Ctrl: 0.242 ± 0.026, n = 162 neurons; 2 h Blue BIC: 0.466 ± 0.028, n = 213 neurons; 4 h Blue TTX: 0.206 ± 0.038, n = 190 neurons; 4 h Blue Ctrl: 0.501 ± 0.110, n = 164 neurons; 4 h Blue BIC: 0.857 ± 0.148, n = 284 neurons from three independent cultures. G/R was analyzed with one-way-ANOVA ($P < 0.001$). $^{**}P < 0.01$ and $^{***}P < 0.001$, Bonferroni *post hoc* significance. Error bars represent s.e.m. (**e**) Cumulative plot of the G/R ratio. When the duration of light illumination is prolonged, larger populations of neurons display higher EGFP expression level. (**f**) Schematic drawing of experimental procedures. (**g**) Representative images of gene expression at each condition. tdTomato is a transfection marker and EGFP is a Cal-Light reporter. Scale bar, 100 μm. (**h**) Average box plot chart of gene expression. The G/R ratio values from individual neurons and a summary box plot chart are superimposed. Dark: 0.11 ± 0.12, n = 86 cells/3 independent cultures; Light only: 0.23 ± 0.14, n = 127 cells/4 cultures, P = 0.27; Activity (three trains) only 0.27 ± 0.14, n = 158 cells/5 cultures; Light + Activity (three trains): 0.58 ± 0.39, n = 263 cells/5 cultures, $P < 0.005$. Boxes show the median, 25th and 75th percentiles and whiskers show min to max.

the fragments to regain protease activity. However, the restored TEV protease cannot recognize TEVseq easily because we replaced the C-terminal end of the Jα-helix of AsLOV2 with TEVseq, preventing TEV protease access in the dark state[17]. In the presence of blue light, Jα-helix is released from the Per-ARNT-Sim core domain of AsLOV2. TEVseq localized at the tip of Jα-helix then becomes easily recognized by the TEV protease, leading to tTA release. Released tTA goes into the nucleus and initiates gene transcription of a target reporter (**Fig. 1a**). Thus, Cal-Light translates neuronal activity into gene expression in a light-dependent manner.

We transfected TM-CaM-TEV-N-AsLOV2-TEVseq-tTA, M13-TEV-C, and TetO-EGFP into hippocampal culture neurons (1:1:0.5 ratio). To increase overall neuronal activity, we blocked GABAA receptors using 30 μM bicuculline (**Fig. 1b**). Despite increased excitability, the expression level of reporter-enhanced green fluorescence protein (EGFP) did not increase in the dark condition; instead, the level was similar to that when neuronal activity was blocked by 2 μM tetrodotoxin (**Fig. 1c**). This result indicates that activity alone cannot initiate gene expression. EGFP expression gradually increased when blue light was turned on for longer periods (1 s ON/9 s OFF for 1, 2, or 4 h) (**Fig. 1d,e**). To determine the minimal amount of time required to drive substantial labeling, we varied light exposure time and intervals. We found that 1 s ON/29 s OFF for 30 min was sufficient to increase the green/red (G/R) ratio significantly, $P < 0.001$ where net light exposure time was just 1 min (**Supplementary Fig. 3a**). We also found that the time interval was not so critical because 3 or 9-s intervals showed similar levels of brightness (**Supplementary Fig. 3a**). Thus, Cal-Light-mediated labeling is more affected by the number of repetitions than by the duration of each light pulse. Brightness of EGFP was also proportionally increased by the light intensity (**Supplementary Fig. 3b,c**). Because Cal-Light requires two components to make gene expression, the stoichiometry of these two components may be critical. We transfected DNA with different ratio as follows; TM-CaM-TevN-AsLOV2-tTA/M13-TevC; 8:1, 3:1, 1:3, or 1:8. We found that when expression of one component considerably exceeded that of the other component, the G/R ratio significantly $P < 0.001$ decreased (**Supplementary Fig. 4**). These results suggest that excessive amount of one component probably increases Ca^{2+} buffering[18]. For example, when the transfection ratio is 8:1, in the presence of neuron-derived Ca^{2+}, endogenous M13 will preferentially bind to TM-CaM-TevN-AsLOV2-tTA. Then, exogenously added M13-TevC has a lower chance of binding TM-CaM-TevN-AsLOV2-tTA, resulting in less tTA release. In contrast, when the transfection ratio is 1:8,

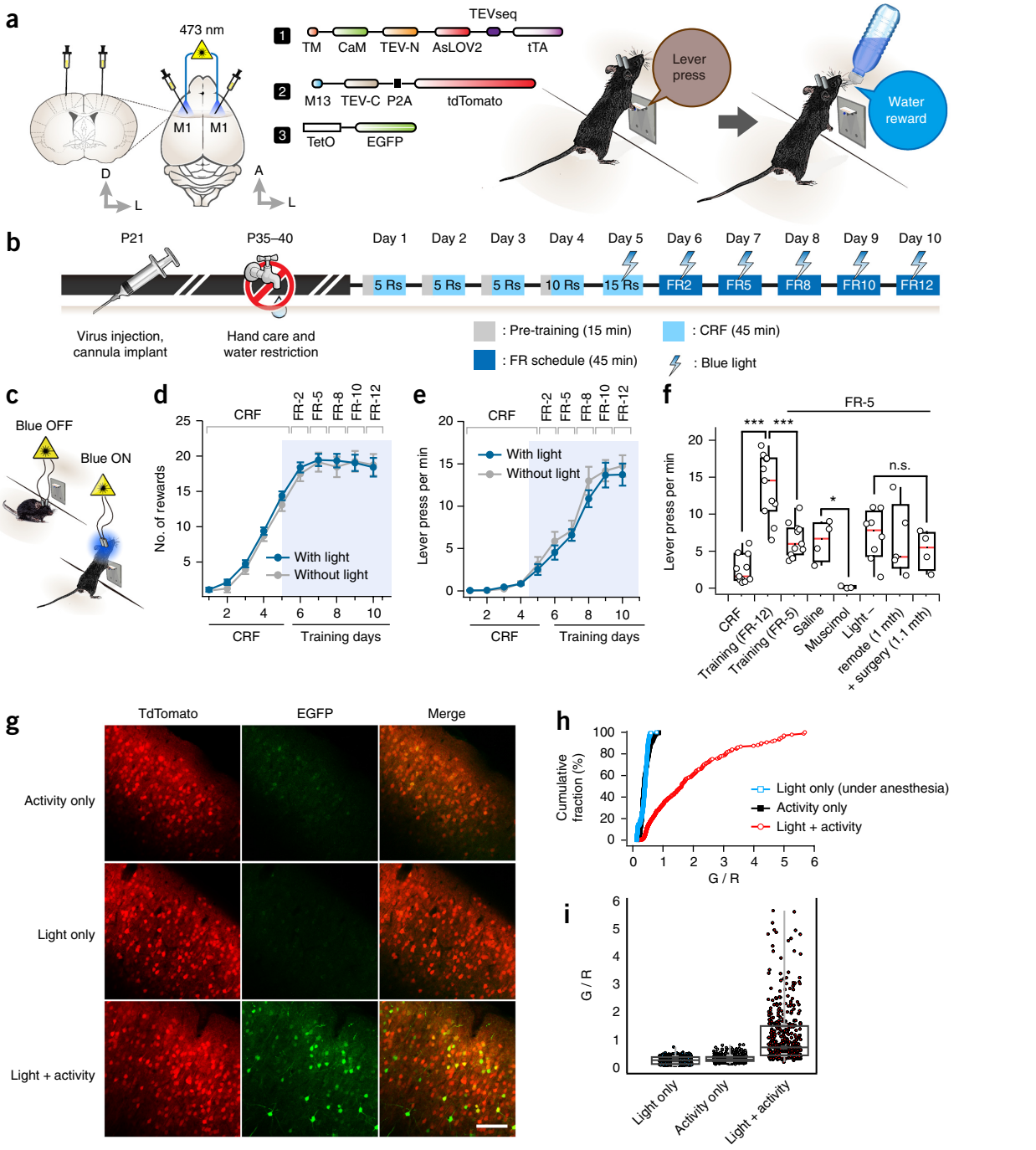

Figure 2 Labeling active population of neurons during complex behavior. (**a**) Bilateral injection of Cal-Light viruses in M1 area. To label learning-related neuronal population, we trained water-restricted mice to learn repetitive lever-pressing behavior to get water rewards. (**b**) Schematic mouse training schedule and Cal-Light labeling with blue light. (**c**) Fiber optics were implanted in both hemispheres of M1 area and blue laser was programmed to be switched on for 5 s whenever mice pressed the lever. Once light was on for 5 s, the next blue light was prohibited for the following 25 s even if mice pressed the lever. (**d**) Number of rewards were gradually increased during learning. Lever press-learning was the same regardless of blue light (8 mice trained without light, 11 mice trained with light). Shaded blue box indicates labeling sessions by blue light. (**e**) The total number of lever presses per minute was also significantly (2.5 ± 0.6, 11 mice; 13.7 ± 1.3, 11 mice, $P < 0.005$) increased while mice were under training (8 mice trained without light, 11 mice trained with light). (**f**) Summary graph of lever presses per minute at different conditions. Note that the number of lever presses was significantly reduced by muscimol injection at M1 region. Lever press-learning was not impaired after one month or together with fiber-optic implantation surgery (continuous reinforcement, CRF: 2.5 ± 0.6, 11 mice; fixed ratio, FR-12: 13.7 ± 1.3, 11 mice, $P < 0.005$; FR-5: 6.6 ± 0.7, 11 mice, $P < 0.005$; Saline: 6.4 ± 1.3, 4 mice; Muscimol: 0.12 ± 0.09, 3 mice, $P < 0.05$; Light–: 7.1 ± 1.2, 8 mice; Remote: 6.4 ± 2.1, 5 mice; Remote + Surgery: 5.1 ± 1.3, 4 mice). Two-sample *t*-test. (**g**) Representative images from mouse brains trained with or without blue light. Scale bars, 100 μm. (**h**) Cumulative distribution of the G/R ratio at each condition (Light only: $n = 448$ cells/8 mice; Activity only: $n = 585$ cells/9 mice; Light + Activity: $n = 504$ cells/11 mice). (**i**) Summary box plot chart of G/R (Light only: 0.32 ± 0.09, $n = 448$; Activity only: 0.36 ± 0.11, $n = 585$, $P = 0.34$; Light + Activity: 1.1 ± 0.97, $n = 504$, $P < 0.005$). $^*P < 0.01$, $^{**}P < 0.05$ and $^{***}P < 0.005$. Error bars in **d** and **e** represent s.e.m. Boxes show the median, 25th and 75th percentiles and whiskers show min to max in **f** and **i**. Two-sample *t*-test.

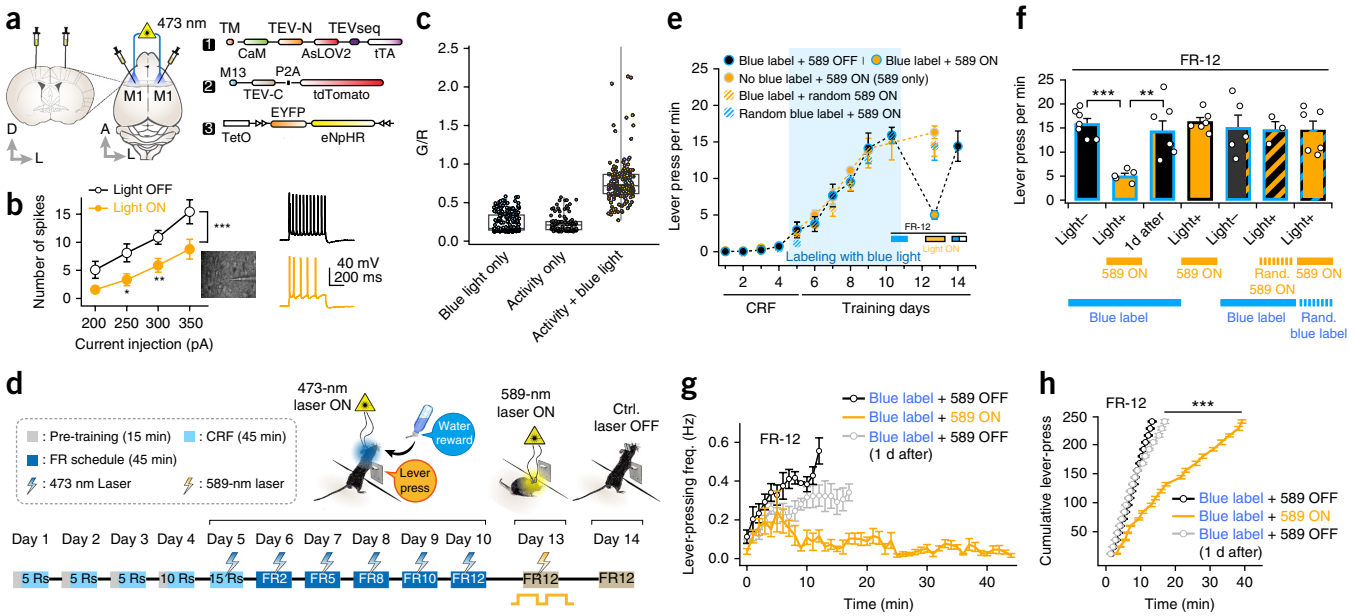

Figure 3 *In vivo* manipulation of learning-related neuronal population. (**a**) Cal-Light viruses were injected into M1 bilaterally. An eNpHR reporter was injected to inhibit activity from selective neuronal population labeled during lever-pressing behavior. (**b**) 589-nm light efficiently inhibited neuronal activity. APs were measured in a current clamp mode before and after 589-nm light from eNpHR-expressing neurons. Average number of APs and representative traces were displayed. Light OFF at 350 pA, 15.4 ± 2.1, $n = 9$; Light ON at 350 pA, 8.8 ± 1.8, $n = 9$, $P < 0.005$. (**c**) Either light or activity alone did not cause high eNpHR reporter gene expression. The G/R ratio from individual neurons were plotted in a box-whisker graph (Blue light only: 0.24 ± 0.12, $n = 228$; Activity only: 0.23 ± 0.11, $n = 115$, $P = 0.56$; Light + activity: 0.79 ± 0.43, $n = 165$, $P < 0.005$). Boxes show the median, 25th and 75th percentiles and whiskers show min to max. (**d**) Illustration of experimental procedures. Neuronal population related to successive lever-pressing learning was labeled by blue light and the learned behavior was selectively inhibited by yellow light. (**e**) Summary learning curve plotted by the number of lever presses per minute. Each group of mice were symbolized by different colors or shapes. "589 only" indicates a mouse group who received the same number and duration of yellow light, but not labeled by blue light. (**f**) Average numbers of lever press per minute at different experimental conditions were plotted. Blue label + 589 OFF: 15.9 ± 1.1, $n = 7$; Blue label + 589 ON: 5.1 ± 0.6, $n = 5$, $P < 0.005$; Blue label + 589 OFF (1 d after): 14.4 ± 2.1, $n = 7$, $P < 0.01$ compared to Blue label + 589 ON; No Blue label + 589 ON (589 only): 16.3 ± 0.9, $n = 6$; Blue label + 589 OFF: 15.1 ± 2.6, $n = 5$; Blue label + Random 589 ON: 14.7 ± 1.7, $n = 3$, $P = 0.884$ compared to Blue label + 589 OFF; Random Blue label + 589 ON: 14.4 ± 1.9, $n = 6$, $P = 0.5$ compare to Random Blue label + 589 OFF (15.9 ± 1.1, $n = 6$, not shown in a graph). (**g**) The frequency of lever-pressing behavior over time. (**h**) Cumulative lever-press number over time. Blue label + 589 OFF: 13.3 ± 1.1 min to reach 240 lever press, $n = 7$; Blue label + 589 ON: 39.2 ± 2.9, $n = 5$; Blue label + 589 OFF (1 d after): 16.9 ± 3.1, $n = 6$, $P < 0.005$ compared to Light OFF. $^{**}P < 0.01$ and $^{***}P < 0.005$. Error bars represent s.e.m. except for **c**. Kolmogorov–Smirnov test.

the exogenously transfected CaM (TM-CaM-TevN-AsLOV2-tTA) will bind Ca^{2+} and interact with the M13-TevC. In this situation there is less M13-TevC and gene expression level decreases. Alternatively, a reduction of the G/R (G: EGFP as a reporter, R: tdTomato as a transfection marker) ratio may be explained by the high amount of tdTomato expression (**Supplementary Fig. 4**). Thus, Cal-Light works the best when the two components are expressed at similar amounts. To determine the portion of EGFP expression induced by the Ca^{2+} rise, we transfected an M13 deletion mutant (TEV-C only) (**Supplementary Fig. 5**). In this case, the expression level did not differ from that in the dark or tetrodotoxin condition, suggesting that only a low level of EGFP expression (G/R fluorescence ratio ranging from 0 to 0.3) arose independently from neuronal activity. Thus, high-EGFP-expressing neurons (G/R ≥ 0.5) are likely to represent meaningful signals triggered by enhanced neuronal activity. To determine the level of potential gene expression caused by lasting effects of blue light or Ca^{2+}, we separated the induction time. We shined the blue light for 2 h and then incubated neurons in the presence of 30 μM bicuculline for 2 h without blue light exposure (light → activity), and performed the opposite experiment (activity → light) as well. When we provided light before increasing activity, almost no EGFP was expressed; in contrast, when we increased activity first there was a slight increase in EGFP gene expression (**Supplementary Fig. 6**). The latter result may be due to some residual activity shortly after the light was turned on. Altogether, these results suggest that Cal-Light is an effective coincident detector of Ca^{2+} and light.

We next verified light and Ca^{2+} dependency in cortical slice cultures by using electrical stimulation. We prepared three groups of slices: light only, activity only, or light and activity (**Fig. 1f**). We repeated one or three trains of action potentials (APs) (each train, 10 pulses at 20 Hz) per minute thirty times. In other groups, AP number at each train was reduced to three or just one pulse. Blue light or activity alone did not significantly increase EGFP expression ($P = 0.27$ for light only and $P = 0.09$ for three trains activity only). A single AP per minute in the presence of light was also not sufficient to increase EGFP expression significantly compared to the light only condition ($P = 0.13$).

However, we observed a significant increase of EGFP expression when AP numbers were increased in the presence of light ($P < 0.05$) (**Fig. 1g,h**). We tested whether Cal-Light-transfected neurons might be more excitable, causing brighter EGFP signals, but did not observe a difference in intrinsic excitability between Cal-Light-positive and Cal-Light-negative neurons (**Supplementary Fig. 7**).

When we injected Cal-Light viruses in striatum *in vivo*, we were able to visualize medium spiny neurons and clear direct and indirect striatal pathways (**Supplementary Fig. 8**). Light-dependent gene expression was also observed in the motor cortex, too (**Supplementary Fig. 9**). Hence, Cal- Light reliably labeled an active population of neurons in a light-dependent manner both *in vitro* and *in vivo*.

To determine if the Cal-Light technique can be used to label a learning-related neuronal population in freely behaving animals, we trained mice in patterned lever pressing[19]. This successive lever-pressing behavior is ideal to test Cal-Light because current techniques, such as methods that detect IEGs, have not been able to label neural circuits responsible for temporally locked motor behaviors. We bilaterally injected Cal-Light viruses into layer 2/3 of the primary motor cortex (M1; **Fig. 2a**). During the first few days of continuous reinforcement, water-restricted mice quickly learned that lever-pressing actions were associated with water rewards (**Fig. 2b**). Once mice learned the link between lever pressing and water rewards, we used fixed-ratio training to progressively increase the required number of lever presses to 12 (**Fig. 2b**). During these sessions, blue light was synchronously illuminated with the first lever-pressing action, thus labeling the neuronal population responsible for successive lever-pressing behaviors (**Fig. 2c**). All mice reliably learned lever-pressing behaviors, as indicated by an increase in the number of rewards and lever presses per minute (**Fig. 2d**,**e**).

The learning curve was similar whether or not we used blue light, demonstrating that blue light itself did not cause any behavioral changes (**Fig. 2d**,**e** and **Supplementary Fig. 10**). To determine whether M1 layer 2/3 neurons are critical for lever-pressing learning, we injected muscimol, a $GABA_A$ receptor agonist, to inhibit neuronal activity or saline into the M1 area of well-trained mice; only the muscimol-injected group showed complete loss of lever-pressing behaviors (**Fig. 2f**). This lever-pressing learning was long-lasting, with the learned behavior still maintained about 1 month later and even after fiber-optic implantation surgery (**Fig. 2f**).

Three days after the last blue light exposure, we examined the expression levels of tdTomato and EGFP in the M1 area. The mouse group trained with no light (activity only) showed robust tdTomato but minimal EGFP expression, confirming that Cal-Light is light-dependent (**Fig. 2g–i**). We anesthetized mice to reduce neuronal activity (**Supplementary Fig. 11**)[20] and delivered the same duration of light to compare light-induced EGFP expression. Similar to our *in vitro* data, EGFP expression was very low, indicating that light alone cannot induce gene expression *in vivo* (**Fig. 2g–i**). Only the mouse group that received blue light during normal training had neurons expressing robust EGFP (**Fig. 2g–i**). We counted putative excitatory pyramidal neurons and interneurons by their morphology or *post hoc* antibody staining; the majority were pyramidal neurons, but the brightest neurons at each slice generally displayed interneuron morphology (**Supplementary Fig. 12** and **Supplementary Video 1**). Quantification data showed that somatostatin (SOM)-positive interneurons were labeled more strongly than other parvalbumin (PV)-positive or vasoactive intestinal polypeptide (VIP)-positive neurons, and a greater number of VIP neurons were Cal-Light-positive (**Supplementary Fig. 13**). To test whether these differential labeling patterns are learning-specific, we performed similar experiments in slice culture. When different types of neurons were activated by channelrhodopsin 2 (ChR2), a similar pattern was observed. SOM-positive neurons showed the highest gene expression level. This robust gene expression was not merely due to a higher firing rate, because PV-positive neurons had a much higher firing rate than SOM neurons (**Supplementary Fig. 14**). Thus, Cal-Light-mediated labeling seemed to be weaker in PV neurons, possibly because PV neurons have higher Ca^{2+} buffering. Altogether, these results suggest that Cal-Light allows access to a subpopulation of pyramidal neurons and interneurons, and enables the study of selective connectivity between different learning-related cell types.

The Cal-Light links gene expression with activity and light, enabling the causal effects of labeled circuits to be testable by optogenetic effectors. To test whether a specific labeled neuronal population is necessary for lever-pressing learning, we injected Cal-Light viruses with a halorhodopsin (eNpHR; enhanced *Natronomonas pharaonis* halorhodopsin) reporter with the goal of silencing neuronal activity (**Fig. 3a**). We first verified that 589-nm yellow light diminished AP firing from eNpHR-expressing neurons (**Fig. 3b**). eNpHR reporter expression also showed dependency on neuronal activity and blue light (**Fig. 3c**). We shined yellow light to suppress the activity of labeled neurons (**Fig. 3d**) and found that pulses of 589-nm yellow light (2 s ON/1 s OFF) during the 45-min probe test strongly inhibited the learned lever-pressing behavior (**Fig. 3e**,f, **Supplementary Fig. 2g–i** and **Supplementary Video 2**) indicating that labeled neurons were learning-related. One day later, lever-pressing behaviors were restored in the same mice that showed severe inhibition (**Fig. 3e**,**f**). Thus, behavioral inhibition was not due to phototoxicity-induced tissue damage or changes in long-term circuit connectivity. Using the same yellow light protocol on a group of mice whose active neurons were not labeled with blue light did not reveal any behavioral impairment (**Fig. 3e**,**f**). This result indicates that yellow light itself does not affect mouse behaviors. Randomized intermittent yellow light (5 s ON/various intervals), desynchronized with lever-pressing behaviors, did not significantly reduce the learned behavior, indicating that inhibiting neuronal activity during lever-pressing is critical (**Fig. 3e**,**f**). In another control mouse group, we shined blue light when mice were walking around in a chamber to label a random population of neurons; pulses of 589-nm light (2 s ON/1 s OFF) during the 45 min probe test did not impair lever-pressing behaviors (**Fig. 3e**,**f** and **Supplementary Video 3**). As an indication of learned behavior, lever-pressing frequency and inter-reward interval were also analyzed (**Fig. 3g**,**h** and **Supplementary Fig. 15**). Altogether, our results show that Cal-Light selectively labels learning-related behaviors with high temporal resolution.

Thus, we demonstrated that the Cal-Light technique reliably transformed transient neuronal activity into gene expression with a high spatiotemporal resolution in freely behaving animals. This technique offers an opportunity to dissect the neural circuits underlying complex behaviors, sensation, and cognitive functions.

METHODS

Methods, including statements of data availability and any associated accession codes and references, are available in the online version of the paper.

Note: Any Supplementary Information and Source Data files are available in the online version of the paper.

ACKNOWLEDGMENTS

We would like to thank B. Kuhlman (University of North Carolina, Chapel Hill) for iLID construct; K. Deisseroth (Stanford University) for an eNpHR-EYFP construct; C. Tucker (University of Colorado) for CRY2 and CIBN constructs; H. Zeng (Allen institute) for a TetO-EGFP construct; S-Y. Choi (Chonnam National University, Republic of Korea) for a P2A vector; W. Weber (University of Freiburg, Germany) for a pSAM200 vector. We thank K-S. Lee and D. Fitzpatrick for helping 3D reconstruction of neurons. We thank M.J. Yetman and H. Taniguchi for helping antibody staining and resource sharing. We thank Y. Chen and B.L. Sabatini for testing initial Cal-Light constructs. We thank all members of the laboratory for critical discussion and comments. This work was supported by funding from a Korea University Grant (to D.L.) and Max Planck Florida Institute for Neuroscience (to H.-B.K.). DNA plasmids used in this study have been deposited to Addgene (Deposit number: 74208).

AUTHOR CONTRIBUTIONS

D.L. and H.-B.K. conceived and initiated the project. D.L. designed and made DNA constructs. D.L. performed *in vitro* characterization and verification in dissociated culture neurons. J.H.H. performed electrophysiological recording and imaging experiments in organotypic slice culture. J.H.H. performed virus injection and all *in vivo* experiments including behavioral training, optogenetic manipulation,

histology, and data analysis. J.H.H. performed electrophysiology recording and 3D reconstruction. K.J. performed *in vivo* calcium imaging in the motor cortex. P.H. helped carry out virus injection, behavioral training, and brain fixation. D.L., J.H.H., K.J., and H.-B.K. wrote the manuscript. All authors discussed and commented on the manuscript.

COMPETING FINANCIAL INTERESTS

The authors declare competing financial interests: details are available in the online version of the paper.

1. Barth, A.L. Visualizing circuits and systems using transgenic reporters of neural activity. *Curr. Opin. Neurobiol.* **17**, 567–571 (2007).
2. Bito, H., Deisseroth, K. & Tsien, R.W. Ca2+-dependent regulation in neuronal gene expression. *Curr. Opin. Neurobiol.* **7**, 419–429 (1997).
3. Flavell, S.W. & Greenberg, M.E. Signaling mechanisms linking neuronal activity to gene expression and plasticity of the nervous system. *Annu. Rev. Neurosci.* **31**, 563–590 (2008).
4. Garner, A.R. *et al.* Generation of a synthetic memory trace. *Science* **335**, 1513–1516 (2012).
5. Inoue, M. *et al.* Synaptic activity-responsive element (SARE): A unique genomic structure with an unusual sensitivity to neuronal activity. *Commun. Integr. Biol.* **3**, 443–446 (2010).
6. Kawashima, T. *et al.* Functional labeling of neurons and their projections using the synthetic activity-dependent promoter E-SARE. *Nat. Methods* **10**, 889–895 (2013).
7. Liu, X. *et al.* Optogenetic stimulation of a hippocampal engram activates fear memory recall. *Nature* **484**, 381–385 (2012).
8. Okuno, H. *et al.* Inverse synaptic tagging of inactive synapses via dynamic interaction of Arc/Arg3.1 with CaMKIIβ. *Cell* **149**, 886–898 (2012).
9. Smeyne, R.J. *et al.* fos-lacZ transgenic mice: mapping sites of gene induction in the central nervous system. *Neuron* **8**, 13–23 (1992).
10. Sørensen, A.T. *et al.* A robust activity marking system for exploring active neuronal ensembles. *eLife* **5**, e13918 (2016).
11. Greer, P.L. & Greenberg, M.E. From synapse to nucleus: calcium-dependent gene transcription in the control of synapse development and function. *Neuron* **59**, 846–860 (2008).
12. Fields, R.D., Eshete, F., Stevens, B. & Itoh, K. Action potential-dependent regulation of gene expression: temporal specificity in ca2+, cAMP-responsive element binding proteins, and mitogen-activated protein kinase signaling. *J. Neurosci.* **17**, 7252–7266 (1997).
13. Fosque, B.F. *et al.* Neural circuits. Labeling of active neural circuits in vivo with designed calcium integrators. *Science* **347**, 755–760 (2015).
14. Kennedy, M.J. *et al.* Rapid blue-light-mediated induction of protein interactions in living cells. *Nat. Methods* **7**, 973–975 (2010).
15. Motta-Mena, L.B. *et al.* An optogenetic gene expression system with rapid activation and deactivation kinetics. *Nat. Chem. Biol.* **10**, 196–202 (2014).
16. Harper, S.M., Neil, L.C. & Gardner, K.H. Structural basis of a phototropin light switch. *Science* **301**, 1541–1544 (2003).
17. Guntas, G. *et al.* Engineering an improved light-induced dimer (iLID) for controlling the localization and activity of signaling proteins. *Proc. Natl. Acad. Sci. USA* **112**, 112–117 (2015).
18. Miyawaki, A., Griesbeck, O., Heim, R. & Tsien, R.Y. Dynamic and quantitative Ca2+ measurements using improved cameleons. *Proc. Natl. Acad. Sci. USA* **96**, 2135–2140 (1999).
19. Jin, X. & Costa, R.M. Start/stop signals emerge in nigrostriatal circuits during sequence learning. *Nature* **466**, 457–462 (2010).
20. Makino, H. & Komiyama, T. Learning enhances the relative impact of top-down processing in the visual cortex. *Nat. Neurosci.* **18**, 1116–1122 (2015).

ONLINE METHODS

Design and construction of plasmid vectors. DNA and amino acids sequence of constructs used in this study are fully described in **Supplementary Sequence**. Briefly, to generate CMV::TM-CaM-NES-TEV-N-AsLOV2- TEVseq-tTA, we amplified CaM, AsLOV2, and tTA sequences from GCaMP6s (gift from Dr. Douglas Kim, Addgene #40753), pLL7.0: Venus-ILID-CAAX (gift from Dr. Brian Kuhlman, Addgene #60411), and pSAM200 (kind gift from Dr. Wilfried Weber, University of Freiburg, Germany), respectively. TM, NES, TEV-N, and TEVseq sequences were synthesized from Eurofin Genomics. Amplified PCR products were digested by suitable combination of restriction enzymes and each PCR product was sub-cloned into pCMV backbone vector. pCMV::M13-TEV-C-P2A-tdTomato was produced by ligating synthesized TEV-C backbone and amplified M13 sequence from GCaMP6s (gift from Dr. Douglas Kim, Addgene #40753). TEV-C sequence was synthesized from Eurofin Genomics. For the generation of reporter AAV vector, pTRE-FLEX- EGFP-WPRE-bGHpA (gift from Dr. Hongkui Zeng, Addgene #65449) was used. Floxed- eNpHR-EYFP sequence were acquired from pAAV-double floxed-eNpHR-EYFP-WPRE-pA (gift from Dr. Karl Deisseroth, Addgene #20949). All plasmid vectors were confirmed by double-strand DNA sequencing (Eurofin Genomics).

HEK293T cell culture and DNA transfections. HEK293T cells were acquired from the American Type Culture Collection (ATCC, Manassas, VA, USA) and had checked the contamination of mycoplasma. HEK293T cells were grown in high glucose Dulbecco's Modified Eagle Medium (DMEM) (Gibco, CA, USA) supplemented with 10% FBS (Cat# 10438-018, Gibco) and 1% penicillin-streptomycin (Invitrogen, NY, USA). Cells were incubated in 37 °C temperature and 10% CO2 conditions. For the experiment, dissociated Cells were plated with 2×10^5 cells per 12 mm coverslip. DNA plasmid vectors were transfected using the Calcium phosphate transfection kit (Clontech, CA, USA). Mixture of DNA solution was slowly added into 2× HEPES Buffered Saline. After 1 h incubation, precipitated solutions were added into each wells. Cell media was replaced 1 d later.

Preparation of dissociated hippocampal culture and DNA transfections. Rat hippocampal neuronal culture was carried out as previously described[21]. Briefly, pregnant CD IGS rat (embryonic 18 day) (Charles River, strain code 001) was rapidly euthanized and hippocampus of embryo were dissected. After 10 min incubation with 0.25% trypsin-EDTA (Invitrogen), trypsinized cells were carefully triturated with 1,000 µL-sized pipet tip ten times. Dissociated cells were plated with 10^5 cells onto 12-mm PDL-coated coverslips. Neurobasal medium (Invitrogen) was used for culture media supplemented with following reagents; 1% (v/v) FBS, 1% (v/v) Glutamax Supplement (Gibco), 2% (v/v) B27 supplement (Gibco), and 1% (v/v) penicillin-streptomycin. Primary hippocampal neuron culture was grown in 37 °C temperature and 10% CO_2 conditions. Every 3~4 d, one-third volume of media were replaced with fresh media lacking FBS. For DNA transfection, modified calcium phosphate transfection method was used as previously described[22].

Blue light illumination to culture neurons. Blue light was illuminated using blue LED panel with 465-nm wavelength (LED wholesalers, Hayward, CA, USA) under the control of high-accuracy digital electronic timer (Model 451, GraLab, Centerville, OH, USA). For the long-term illumination, LED panel was installed inside of CO_2 incubator. One transparent 6-well plate with 2-cm height was installed between the LED panel and sample plate to inhibit undesirable heating effect by the direct contact of LED. In this experimental setup, the light intensity of blue LED was 1.7 mW, measured by a power meter (PM100D, Thorlabs, Newton, NJ, USA). To prevent room light, all sample plates were wrapped with aluminum foil, and every experimental procedure was carried out under dim red light.

Animals. For lever-pressing behavior training, C57BL6J mice were purchased (3- to 8-weeks old, either sex, Jackson Laboratory, Bar Harbor, ME, USA). All mice were individually housed in a day and night reverse cycle room and all behavioral experiments were performed during day period. Mice were water restricted to 1 ml water per day for 3 d before training starts. Mice had free access to food *ad libitum*. Animals that went to experimental or control group were randomly selected. Behavioral training was not performed in a blinded fashion. All experimental procedures and protocols were approved by the Institutional Animal Care and Use Committee and National Institutes of Health guidelines.

Animal surgery and stereotactic viral injection. The cocktail of ketamine (0.1 mg/g) and xylazine (0.01 mg/g) (Sigma-Aldrich) was used to anesthetize mice via intraperitoneal injection. Hair was shaved by Nair (Church & Dwight Co., Inc.; Princeton, NJ, USA) and petrolatum ointment (Puralube Vet Ophthalmic Ointment) was applied to both eyes to prevent dryness of eyes. The head was fixed to stereotactic device (Kopf instruments, Tujunga, CA, USA) by ear bars and a nose clamp. Surgical region was sterilized with alcohol and 10% betadine solution (Purdue product LP, Stamford, CT, USA). During surgery, body temperature was maintained constantly at 37 °C using a homeothermic blanket with flexible probe (Harvard Apparatus, Holliston, MA, USA). Head skin and periosteum were carefully removed by a sharp surgical scissor and scalpel maintained in aseptic surgical conditions. To make small burr hole (~0.5 mm in diameter) on each hemisphere, we used a hand- held drill (Fordom Electric Co., Bethel, CT, USA) under the surgical microscope. To target M1 area, glass micropipettes (tip size 10–20 µm diameter, Braubrand) containing AAV-viral solution was lowered to 300 µm beneath from the surface of brain and retracted the pipette a little bit to the final target site (final target site: AP, +0.25 mm; ML, +1.5 mm from bregma, and DV −0.2 mm from the brain surface). 600–750 nl of virus containing solution (AAV1-hSYN-TM-CaM- TEV-N-AsLOV2-TEVseq-tTA: AAV1-hSYN-M13-TEV-C-P2A-tdTomato: AAV1-TRE-EGFP = 1: 1: 2) was injected into primary motor cortex (M1) area, at the speed of 100~200 nl/min. After injection, micropipette was hold for 3 min to prevent backflow of viral solutions. We determined the final injection coordinates through several injection trials using a fast green dye and the reference of mouse brain atlas[23] (G. Paxinos and K. Franklin, Academic press).

Fabrication and implantation of optic fiber. An optic fiber (low OH, 200 µm core, 0.37 NA; Cat# BFL37-2000, Thorlabs) was cut with a diamond knife and inserted into the 1.25 mm diameter of ceramic ferrule (Cat# CFLC230-10, Thorlabs) with a 230 µm bore. The optic fiber was adhered to a ferrule using epoxy (Gorilla Glue Company, Cincinnati, OH, USA). Both end of optic fibers were finely grinded by using sandpaper and grinding puck (Thorlabs). After viral injection, the optic fiber was implanted perpendicularly into the targeted brain region under the guidance of stereotactic device and a cannula holder (Cat# XCL, Thorlabs). The tip of fiber was positioned 100–150 µm above the target viral injection site in M1 area. In order to secure the implanted optic fiber, dental cement (C&B-Metabond, Parkell Inc, Edgewood, NY, USA) was applied to skull surface. When dental cement was completely solidified, the cannula holder was removed and the hole was covered by a plastic dust cap (CAPL, Thorlabs) to prevent potential light exposure. An analgesic (buprenorphine, 0.05 mg kg^{-1} of body weight) was injected subcutaneously to relieve post-surgical pain and mice were returned back to their home cage for recovery. Light illumination through fiber connectors was pre-tested before implantation. In order to target striatum, 750 nl viral stock solution (AAV1-hSYN-TM-CaM-TEV-N- AsLOV2-TEVseq-tTA: AAV1-hSYN-M13-TEV-C-P2A-tdTomato: AAV1-TRE-EGFP: AAV1-CMV-PI-Cre-rBG: dFlox-ChR2-mCherry = 1: 1: 2: 2: 4) was injected to the dorsal striatum (Coordinates: AP, +1 mm; ML, +1.5 mm from bregma, and DV −2.2 mm from the brain surface). The tip of optic fiber was located at 300–400 µm above from the virus injection site in order to deliver blue light broadly in striatum. Three weeks after viral injection, blue light was delivered (473 nm, 2 s ON, 1 s OFF for 45 min) to striatum while mice are awake. Blue laser (MBL-FN-473, Changchun New Industries Optoelectronics Technology, Jilin, China) was controlled by MED-PC IV software, which connected with an acquisition board (Med- Associates, St. Albans, VT).

Lever-press behavior training. Mice were handled approximately 5 min per day 5–6 d before training started. Training was performed in a standard mouse operant chamber (Med-Associates, St. Albans, VT) placed in sound-attenuating cubicle (ENV-022MD, 22 cm × 15 cm × 16 cm). Each chamber (ENV-307W) was equipped with two retractable levers on either side of the water magazine, and a house light was placed on the opposite side of the magazine. When mice got rewards, they were allowed to lick the water through a

retractable sipper with graduated pipette which extends into the chamber and remains there for 3 or 10 s and then is retracted out of the chamber. Behavioral training in an operant chamber is made of two phases. The first phase of training (on days 1–4) starts with pre-training session (on average of 30 reinforcers delivered randomly over 15 min, magazine training session) followed by the continuous reinforcement (CRF) session, in which a mouse obtains a large reward (sipper tube extends into the chamber for 10 s) after each left- or right-lever press. CRF session lasts 45 min or until mice receive five rewards (CRF 5Rs), and the next day CRF lasted 45 min or until mice received ten rewards (CRF 10Rs). Most mice complete the first phase of training within 4 d. After completing CRF 10Rs, the second phase of training (on days 5–10) starts from CRF 15Rs (in which every response results in small reward (for 3 s) with water; up to 15 rewards within 45 min) without pre-training. And the following day of CRF 15Rs, mice start to be trained on fixed ratio (FR) schedule which consists of FR-2 (two presses to get a reward, regardless of left or right), FR-5, FR-8, FR-10, and FR-12 (lever pressing 12 times to get reward once) for 5 to 7 consecutive days. Mice were given 45 min to earn 20 total water rewards at each session per day. Water was restricted throughout the training periods and mice receive the rest of the water after subtraction of the amount of water given during training to make total 1 ml of water per day.

Optical labeling of the task-related neurons. 473 nm blue light (MBL-FN-473, Changchun New Industries Optoelectronics Technology, Jilin, China) was delivered with a light cycle of 5 s ON and 25 s OFF during the second phase of training (from CRF 15Rs to FR-12). Blue light illumination begins with lever-pressing behavior and lasts for 5 s and next blue light was prohibited for the following 25 s even if mice press the lever again (5 s ON/25 s OFF cycle). Light intensity was adjusted with a power meter (Thorlabs) to reach 10–15 mW measured at the end of the fiber tip. The total duration of blue light was 611.3 ± 198.1 s. The light only control was received blue light for 600 s (5 s ON/25 s OFF, 120 times) under anesthetization.

Behavioral changes by optogenetic inhibition. Mice were allowed to recover from viral injection (AAV1-hSYN-TM-CaM-TEV-N-AsLOV2- TEVseq-tTA: AAV1-hSYN-M13-TEV-C-P2A-tdTomato: AAV1-CMV-PI-Cre-rBG: AAV1-TRE-Flox-eNpHR-EYFP, in a pre-mixed 1:1: 2:4 ratio) and optic-fiber implantation surgery for 18–25 d before training started. Mice were trained for 10 d to reach the FR-12 session. Labeling of the skilled motor learning-related neuronal population was accomplished by the delivery of blue light (473 nm; 10–15 mW) through the bilateral optic fiber from CRF 15Rs to FR-12. For optical inhibition of aforementioned subset of labeled neurons, probe test (589 nm, 2 s ON/1 s OFF for 45 min) was conducted on day 13, 3 d after the last training session. The power of laser was measured at the end of the tip of fiber and adjusted to be 15–20 mW. On the next day, the mice were tested in the same chamber without 593-nm laser. The number of rewards and lever presses per minute were analyzed as behavioral readouts. To determine whether random yellow light during sessions was enough to inhibit skilled lever-pressing behaviors or not, random 589-nm light was generated by using a random number generator function. Yellow light was delivered for 5 s at random intervals of 5, 30, 40, 50 s (average of interval, 31.3 s). The same behavioral outputs were analyzed.

Optical labeling of random population of neurons. Mouse training schedules were identical for random labeling, but blue light was illuminated in a random fashion (independent of lever-pressing behavior). To label learning-irrelevant neuronal population, blue light was shined when mice were not pressing levers. However, it was difficult to find appropriate time window to deliver blue light independent of lever pressing and reward behaviors, because trained mice spent most of their time lever-pressing to get rewards during training sessions. For that reason, to match the total duration of blue light between the test and control mouse groups, the mouse group labeled by random blue light illumination received blue light exposure from day 2 of the first phase of training till day 8. The total duration of blue light was similar (~600 s). The probe behavior test with 589-nm light was same (2 s ON/1 s OFF for 45 min).

Pharmacological silencing of M1 area. 300 nl of muscimol (1 μg/1 μl in ACSF) or the same amount of saline was injected into the trained mice. Injection was made bilaterally in M1 area (AP, +0.25 mm; ML, +1.5 mm from bregma, and DV −0.2 mm from the brain surface) under anesthesia (2% isoflurane). After the surgery, the mice were allowed to recover in their home cage for 30 min before the behavioral test. After mice were fully recovered from anesthetization, the mice were placed in the behavioral chamber and performed lever-pressing tasks for 45 min.

***In vivo* two-photon calcium imaging during awake and anesthetized states.** Surgeries were performed on 4- to 6-week-old mice. Mice were anaesthetized with an intraperitoneal injection of an anesthetic cocktail containing ketamine ($80 mg kg^{-1}$) and xylazine ($12.5 mg kg^{-1}$) (Sigma-Aldrich). The animal's scalp was shaved, any remaining hair was removed with a hair remover lotion (Nair, Church & Dwight Co, Inc; Princeton, NJ, USA) and ophthalmic ointment (Puralube Vet Ophthalmic Ointment) was applied to prevent eyes from drying. Next, the animal was placed in device (Kopf, Model 900 Small Animal Stereotaxic Instrument), and surgical region was scrubbed by 10% betadine solution (Purdue product LP, Stamford, CT, USA). Small incision was made on the scalp and the surface of skull was cleaned. Small craniotomy (~0.5 mm in diameter) was made above the motor cortex and AAV1-hSyn- GCaMP6s-WPRE-SV40 (400 nl, Penn Vector Core) was injected into layer 2/3 motor cortex via a beveled glass micropipette (tip size 10–20 μm diameter, Braubrand) backfilled with mineral oil. Flow rate ($100 nl min^{-1}$) was regulated by a syringe pump (World Precision Instruments). After injection, a micropipette was held for 3 min to prevent a backflow of viral solution. Following virus injection, skin adhesive (3M vetbond) was applied to close the incision site. General analgesia (buprenorphine, 0.05 mg kg^{-1} of body weight) was injected subcutaneously and mice were monitored until they recovered from anesthesia. After around a week later, mice were anesthetized and hair was removed. A scalp was removed in a circular shape and the surface of the skull was cleaned. Cranial window (3 mm diameter) was implemented on the virus injection site and custom-made headplates were attached to the exposed skull with the dental adhesive (C&B-Metabond, Parkell Inc, Edgewood, NY, USA). After 2 weeks of recovery from cranial window surgery, awake mice were head-fixed on the air-supported spherical treadmill and spontaneous neuronal activity of the motor cortex was imaged for 800 s by using a two-photon microscope (Prairie Technologies, Inc). For an anesthetized state, mice were anaesthetized with an intraperitoneal injection of an anesthetic cocktail containing ketamine ($80 mg kg^{-1}$) and xylazine ($12.5 mg kg^{-1}$) and spontaneous neuronal activity of the motor cortex was imaged for 800 s. Imaging data were motion-corrected using a normalized cross-correlation image-registration algorithm in Matlab imaging processing toolbox (Mathworks). Regions of interests (ROIs) were semi-automatically drawn using a cell size, cell shape, and fluorescence intensity. The pixels in each ROI at each imaging frame were averaged to create a fluorescence time series. The surrounding neuropil area was drawn from 0.3 μm outside of each cell's ROI to 10 μm. The neuropil area excluded ROIs of adjacent cells. Pixels in neuropil area showing apparent calcium transients exceeding three times the s.d. of neuropil fluorescence time series. Remaining pixels of neuropil area were averaged to create background neuropil fluorescence trace. The neuropil fluorescence trace was subtracted from fluorescence trace of each neuronal ROI (F). The preliminary baseline ($F0$) of a fluorescence trace was estimated by smoothing over 120 imaging frames. The preliminary baseline ($F0$) was subtracted from the neuronal ROI fluorescence trace (F) to estimate the preliminary ΔF. The preliminary ΔF was Lowess-smoothed over five imaging frames. The noise was estimated as the s.d. of the difference between the preliminary ΔF and the smoothed preliminary ΔF. The offset was then estimated from the mean of Gaussian fit of the distribution of the preliminary ΔF less than two times noise level. The baseline ($F0$) of a fluorescence trace was then estimated by adding the offset to the preliminary baseline ($F0$). $\Delta F/F$ was calculated by subtracting the baseline ($F0$) from the neuronal ROI fluorescence trace (F) and dividing it by the baseline ($F0$).

***Ex vivo* electrophysiology.** Trained C57BL6J mice were deeply anesthetized with isoflurane and they were decapitated. The brain was quickly removed and chilled in ice-cold high-magnesium cutting solution containing the following (in mM): 100 choline chloride, 25 $NaHCO_3$, 2.5 KCl, 0.5 $CaCl_2$, 7 MgCl2, 1.25 NaH_2PO_4, 25 glucose, 20 HEPES, 3.1 Na-pyruvate, 5 Na-ascorbate. pH and osmolarity were adjusted to 7.4 and ~300 mOsm, respectively.

doi:10.1038/nbt.3902

The isolated brain was placed onto the stage of a vibratome (Leica VT1000, Leica Biosystems, Buffalo Grove, IL, USA) and 300 μm-thick coronal cortical slices were cut. The slices were transferred and incubated at 34 °C for 30 min in a slice container superfused with artificial cerebrospinal fluid (ACSF) solution containing the following (in mM): 124 NaCl, 26 $NaHCO_3$, 3.2 KCl, 2.5 $CaCl_2$, 1.3 $MgCl_2$, 1.25 NaH_2PO_4, 10 glucose, saturated with 95% O_2 and 5% CO_2 gas. Thereafter slices were maintained at room temperature for the experiments. For whole-cell voltage- or current-clamp recordings, slices were placed in a recording chamber where ACSF was perfused with a speed of 1–1.5 ml/min. Layer 2/3 cortical neurons (e.g., Cal-Light or EGFP, positive or negative neurons) in M1 were recorded. The recordings were made using a MultiClamp 700B amplifier controlled by Clampex 10.2 via Digidata 1440A data acquisition system (Molecular Devices). The pipette solution was made as follows (in mM): 125 K-gluconate, 5 KCl, 10 Na_2-phosphocreatine, 4 Mg-ATP, 0.4 Na- GTP, 10 HEPES, 1 EGTA, 3 Na-ascorbate (pH = 7.25 with KOH, 295 mOsm). To select EGFP positive neurons labeled by Cal-Light, first tdTomato (expression marker for Cal-Light transfection) positive neurons were identified under 565-nm wavelength LED (pE-100, CoolLED). Then, LED wavelength was switched to 470 nm to confirm whether neurons also express EGFP. In a whole-cell current clamp mode, membrane potential was maintained at −67.5 ± 1.8 mV. Under this condition, we monitored input-output relationship and action potential properties (**Supplementary Figs. 8** and **13**). In **Figure 3b**, step current (500 ms) was injected from 200 pA to 350 pA and the number of spikes were quantified with and without 589-nm laser (CNI, China).

Preparation of cortical organotypic slice culture and virus infection. Organotypic slice cultures were made from P2-P4 C57BL/6 mice (Charles River Laboratory), PV-Cre (Jackson Laboratory, 8069) and SOM-Cre (Jackson Laboratory, 13044). The general procedures for organotypic slice cultures were followed as previously described[24]. Briefly, coronal sections of cortex (thickness, 400 μm) including M1 area were made by a tissue chopper (The Mickle Laboratory Engineering Co. Ltd., UK). The age of culture is indicated by an equivalent postnatal (EP) day; postnatal day at slice culture (P) + days *in vitro* (DIV).

At EP 5–8, individual cultured slices were infected by dropping 5 μl of mixed solution, 1 μl of virus containing solution (titer: ~10^{13}–10^{14} GC/ml) and 4 μl of slice culture media (pre-warmed at 37 °C), to the surface of brain slice placed on porous (0.4 μm) membrane (Millicell-CM; Millipore). For channelrhodopsin-2 expression, AAV1-EF1-dflox-hChR2(H134R)-mCherry-WPRE-hGH (Penn Vector Core) was infected to slice culture from each Cre mouse line. Once viruses were infected, culture plate was covered by aluminum foil to prevent light exposure and maintained at 37 °C. Experiments were performed at EP 20, 2 weeks after viral infection. Cal-Light viral AAV vectors were cloned in the lab and viruses were produced at ViGene Bioscience (Rockville, MD, USA).

Testing activity and light sensitivity in organotypic slice cultures. Concentric bipolar electrodes (12.5 μm inner pole diameter, 125 μm outer pole diameter; FHC Inc.) was positioned at layer 2/3 cortical area. Stimulation pulses (100 μs in duration, stimulus intensity, 10–15 V) were generated by a digital stimulator (Master 8, AMPI, Israel) and fed into the stimulation electrode via an isolation unit (DS2A, Digitimer Ltd). A blue laser (MBL-F-473 nm-200 mW, CNI, China) coupled to a FC/APC fiber (400 μm, 1 m long, CNI) was positioned 2 cm above the surface of the cortical slice. Total power from the tip of the fiber was 5–10 mW. Blue light was illuminated for 30 min (10 s ON / 50 s OFF) with or without electrical stimulation (Light + Activity vs Light only). Three trains of electrical stimulations were delivered per minute. Each train is made of 10 pulses at 20 Hz and repeated three times with an interval 1.6 s. Blue light was delivered 100 ms before the onset of first electrical stimulation of each train and lasted for 10 s.

Tissue fixation, immunohistochemistry, and acquisition of confocal images. Animals were deeply anesthetized by a mixture of ketamine and xylazine and then perfused transcardially, first with PBS (pH 7.4) and next with 4% paraformaldehyde (PFA) dissolved in PBS. The brains were removed and postfixed in 4% PFA overnight at 4 °C. The brains were embedded into 10% melted gelatin solution for 50 min at 50 °C and then gelatin solution was refreshed. Gelatin solution with the embedded brains were kept in 4 °C for ~30 min for solidification of gel. Then the gel was trimmed to a small cube around the brain and the cube was kept in 4% PFA solution overnight. Coronal section (thickness, 100 μm) was made using a vibratome (Leica VT1200) for confocal imaging. For immunohistochemistry, brain slices were incubated with primary antibodies (1:500 mouse anti-parvalbumin, #P3088, Sigma; 1:250 rat anti-somatostatin, Milllipore, #MAB354; 1:500 rabbit anti-VIP, Abcam, #ab43841) for 24 h at 4 °C (48 h for PV). All secondary antibodies were used after diluted to 1:1,000 in PBS (Cy5- conjugated donkey anti–mouse IgG for PV; donkey anti-rat IgG for somatostatin; donkey anti- rabbit for VIP, Jackson ImmunoResearch Laboratories). Imaging was performed using upright confocal laser-scanning microscope (LSM880, Zeiss, Germany) with 20 × /0.8 M27 objective lens. The G/R value of individual cells were analyzed using ImageJ (NIH).

3D reconstruction of the cell. Brain slices are mounted onto slides with PBS. Labeled neurons and structures were viewed on confocal microscopy (Leica TCS SP5 resonant scanning Confocal) with 63 × glycerol immersion objective lens. The neuron was imaged with 5-by-5 tile-scan (X, Y, Z pixel size: 59, 59, 160 nm), approximately 150 μm field of view. Deconvolution was applied to the image with theoretical point spread function for the confocal microscopy (Huygens Software, Scientific Volume Imaging). 3D reconstruction was performed using Neurolucida 360 (MBF Bioscience).

Pharmacology. Bicuculline and tetrodotoxin were purchased from Tocris Bioscience (Minneapolis, MN, USA). All drug stock solution was prepared with 1,000× or greater.

Statistics. Statistical significance of culture neuron data was calculated by one-way ANOVA with *post hoc* Bonferroni test using SPSS 21 (IBM) software. Organotypic slice culture and *in vivo* data ware analyzed using IgorPro (version 6.10A; WaveMetrics, Lake Oswego, OR, USA). Statistical data were presented as means ± standard error of mean (s.e.m., denoted as error bars), and *n* indicates the number of cells or animals studied. The significance of differences between two experimental conditions was evaluated using Student's *t* test, or Wilcoxon's signed rank test for non-paired and paired data after testing normality using the Kolmogorov–Smirnov test. Comparison of the G/R ratio in *in vivo* and *in vitro* slice culture experiments and behavioral changes during lever-press task was evaluated using nonparametric Mann–Whitney *U* test. Difference were considered as significant when $P < 0.05$. n.s., no statistical significance; *, $P < 0.05$, **, $P < 0.01$, ***, $P < 0.005$.

Data availability. Data are available from the corresponding author upon reasonable request

21. Lee, D. *et al.* Inositol 1,4,5-trisphosphate 3-kinase A is a novel microtubule-associated protein: PKA-dependent phosphoregulation of microtubule binding affinity. *J. Biol. Chem.* **287**, 15981–15995 (2012).
22. Jiang, M. & Chen, G. High Ca2+-phosphate transfection efficiency in low-density neuronal cultures. *Nat. Protoc.* **1**, 695–700 (2006).
23. Paxinos, G. & Franklin, K.*The Mouse Brain in Stereotaxic Coordinates* (Elsevier, 2013).
24. Stoppini, L., Buchs, P.A. & Muller, D. A simple method for organotypic cultures of nervous tissue. *J. Neurosci. Methods* **37**, 173–182 (1991).